

Article

Gasification of Shenhua Bituminous Coal with CO₂: Effect of Coal Particle Size on Kinetic Behavior and Ash Fusibility

Jinzh Zhang , Zhiqi Wang ^{*}, Ruidong Zhao and Jinhu Wu

Key Laboratory of Biofuels, Qingdao Institute of Bioenergy and Bioprocess Technology, Chinese Academy of Sciences, Qingdao 266101, China; zjz1988156@gmail.com (J.Z.); zhaord@qibebt.ac.cn (R.Z.); wujh@qibebt.ac.cn (J.W.)

^{*} Correspondence: wangzq@qibebt.ac.cn; Tel.: +86-532-8066-2763

Received: 9 May 2020; Accepted: 2 June 2020; Published: 29 June 2020



Abstract: Coal gasification is the process that produces valuable gaseous mixtures consisting primarily of H₂ and CO, which can be used to produce liquid fuel and various kinds of chemicals. The literature shows that the effect of particle size on coal gasification and fusibility of coal ash is not clear. In this study, the gasification kinetics and ash fusibility of three coal samples with different particle size ranges were investigated. Thermogravimetric results of coal under a CO₂ atmosphere showed that the whole weight loss process consisted of three stages: the loss of moisture, the release of volatile matter, and char gasification with CO₂. Coal is a heterogeneous material containing impurities. Different grinding fineness leads to different liberation degrees for impurities. As for the effect of particle size on TG (thermogravimetry) curves, we found that the final solid residue amount was the largest for the coal sample with the smallest particle size. The Miura-Maki isoconversional model was proved to be appropriate to estimate the activation energy and its value experienced a slow increase when the particle size of raw coal increased. Further, we found that particle size had an important impact on ash fusion temperatures and small particle size resulted in higher ash fusion temperatures.

Keywords: bituminous coal; gasification kinetics; ash fusibility; particle size

1. Introduction

Coal, as a traditional fossil fuel, will continue to be dominant in China's energy sector for a relatively long time [1]. In order to deal with increasing environmental problems, clean and efficient coal conversion technologies must be urgently developed. Coal gasification technology deserves attention because it is the process that produces valuable gaseous mixtures consisting primarily of H₂ and CO (syngas) with high fuel conversion efficiency [2]. Syngas can be utilized to produce liquid fuel and various kinds of chemicals.

Coal gasification contains two primary stages: (1) pyrolysis of raw coal and (2) gasification of remaining coal char [3]. Char gasification is usually a slower process than pyrolysis and is the rate-limiting step of the whole process; therefore, the knowledge of gasification kinetics is vital for designing gasification reactors [2]. Thus, gasification kinetic analyses are the starting point for the design, optimization, and operation of gasifiers [3,4]. The most frequently utilized gasification agents include O₂, air, H₂O, and CO₂, among which steam is the most widely used [2]. Unlike CO₂, water is resource-limited and energy-intensive. Although CO₂ is less reactive than steam, it is still widely used in the coal gasification process because it can reduce the dependence on water resources [5].

Many factors have been proven to affect coal gasification rates, including temperatures [5,6], partial pressure of the gasification agent [5,7], coal rank [8,9], as well as particle size [10,11]. Coal is

a heterogeneous material containing large amounts of impurities, like mineral matter. The fact that the impurities are often finely dispersed in the coal structure or matrix implies that full grinding would result in sufficient liberation. Therefore, it is necessary to decrease the particle size to liberate the mineral matter. The literature has explored the effect of coal particle size on pyrolysis and gasification characteristics [1,11–13]. Liu et al. [14–17] conducted a systematic study of coal pyrolysis characteristics including formation mechanisms of methane, carbon monoxide, nitrogen-containing species, and functionalities in chars using samples with different particle sizes. It was found that the coal particle size influenced the sulfur release behavior by Krishnamoorthy et al. [18]. Jayaraman et al. [19] reported that the TG (thermogravimetry) and DTG (differential thermogravimetric) curves shifted towards a lower temperature zone with the decrease of coal particle size. Furthermore, to the best of our knowledge, little attention has been paid to the effect of particle size on the gasification kinetics in a CO₂ atmosphere, which is absolutely vital for selecting the most suitable coal particle size. Song et al. [11] demonstrated that the larger the particle size, the lower the char reactivity for raw coal. However, Hanson et al. [10] reported that coal particle size had little influence on pyrolysis and the gasification process. It can be seen from the conflicting conclusions that the effect of coal particle size on pyrolysis and gasification characteristics is still unclear.

Variations of the ash component and content often show a distribution with respect to the different coal particle fractions, which consequently affect the coal ash fusibility. Coal ash fusibility is the key parameter related with ash fouling and slagging in the boiler and gasifier. Ash fusibility temperatures (AFTs) are essentially dependent on the chemical compositions of coal ash. There is much less research about the effect of particle size on the fusibility of coal ash under a CO₂ atmosphere.

The primary objective of the present study was to explore the effect of particle size on the gasification kinetic behaviour and ash fusibility using CO₂ as the gasification agent. Three different particle size fractions were screened from Shenhua bituminous coal. The gasification of coal samples was studied experimentally by thermogravimetry. The kinetic parameters of gasification under the CO₂ atmosphere were calculated using the Miura-Maki integral isoconversional model.

2. Materials and Methods

Bituminous coal obtained from the Shenhua mine was used in this study. The coal sample was ground by a ball mill and the coal samples with different particle size ranges were obtained by screening. In order to investigate the effect of particle size on pyrolysis and gasification behavior, this work used three coal samples with different particle size ranges labelled as sample 1#, sample 2#, and sample 3#, respectively. The properties of the three coal samples are given in Table 1. The information about the particle size was determined by a Malvern Mastersizer 3000.

Table 1. Proximate and ultimate analysis of the coals.

Sample	Proximate Analysis (ad, %)				Ultimate Analysis (daf, %)				
	M	A	V	FC *	C	H	N	S	O *
1#	6.11	15.24	28.04	50.61	89.22	4.67	1.04	1.24	3.83
2#	6.80	9.91	27.86	55.43	84.26	7.53	1.07	1.03	6.10
3#	7.30	11.10	28.15	53.45	82.40	8.09	1.12	1.44	6.95

Note: ad, air dried; daf, dry and ash free basis; M, moisture; A, ash; V, volatiles; FC, fixed carbon; *, calculated by difference; C, carbon; H, hydrogen; N, nitrogen; S, sulphur; O, oxygen.

A thermogravimetric analysis was conducted with a TG (Setsys Evolution, SETARAM, France in Shanxi Institute of Coal Chemistry, Chinese Academy of Sciences). In each experiment, about 10 mg of coal was used in order to eliminate the effects of internal diffusion. Every sample was heated under a CO₂ atmosphere from an ambient temperature of 1300 °C with four different heating rates (5, 10, 20, and 40 °C/min). The experiment for each particle size was repeated three times to ensure the reliability of the TG curves.

3. Results

3.1. Kinetic Analysis with Miura Isoconversional Method

The model-free method (Equation (1)) is an integral isoconversional model, which was proposed by Miura-Maki [20] to calculate the activation energy at selected conversions. The detailed description of the isoconversional method (also called the distributed activation energy model, DAEM) was reported in our previous papers [21–25]:

$$\ln\left(\frac{\beta}{T^2}\right) = \ln\left(\frac{k_0 R}{E}\right) + 0.6075 - \frac{E}{RT}, \quad (1)$$

where β is the heating rate; k_0 is the pre-exponential factor; E is the activation energy; R is the universal gas constant; T is the absolute temperature (K).

3.2. Ash Fusibility of Shenhua Bituminous Coal

3.2.1. Preparation of the Ash

The ash samples were prepared by ashing the three Shenhua bituminous coal samples in a muffle furnace at 800 °C for 24 h.

3.2.2. XRF Measurements

Chemical analysis was performed by using a wavelength-dispersive sequential X-ray spectrometer (Shimadzu XRF-1800) with an Rh-target X-ray tube, which was operated at 50 kV and 40 mA.

3.2.3. Ash Fusion Temperature Test

The ash fusion temperature test was performed by following the Chinese standard procedures (GB/T219-2008) in a registered independent laboratory. This test involved heating a sample cone of a specified geometry at a heating rate of 15 °C/min to 900 °C and then changing the heating rate to 5 °C/min in a weak-reducing atmosphere by sealing a certain amount of carbon materials in the furnace. The following four specific temperatures have been recorded for each sample: deformation temperature (DT), softening temperature (ST), hemispherical temperature (HT), and flow temperature (FT).

4. Discussion

4.1. Determination of Coal Particle Size

Table 2 shows that the average particle size of 3# was the highest, followed by 2#, and 1# had the lowest average particle size. The particle size distribution results in Figure 1 also supports this conclusion.

Table 2. The characteristic particle size for coal samples used in this work.

	1#	2#	3#
$D_v(50)/\mu\text{m}$	11.7	43.4	132

4.2. Thermal Behavior Based on TG/DTG Curves

The TG and DTG curves of the three coal samples with different particle sizes under the CO₂ atmosphere are shown in Figure 2. It can be seen that there were three significant weight loss peaks. The first small peak in the low temperature range (<200 °C) was due to the loss of moisture. The second weight loss peak in the medium temperature range (around 400–700 °C), which underwent the thermal degradation reactions, released a large amount of volatile matter. The third large weight loss peak in the high temperature range (>720 °C) was evidently attributed to the gasification of coal char with

CO₂. Figure 2 also presents the effects of different heating rates ($\beta = 5, 10, 20,$ and $40\text{ }^{\circ}\text{C}/\text{min}$) on the TG and DTG curves. The weight loss peaks shifted towards the higher temperature range and obvious thermal hysteresis could be observed with the increase of the heating rate.

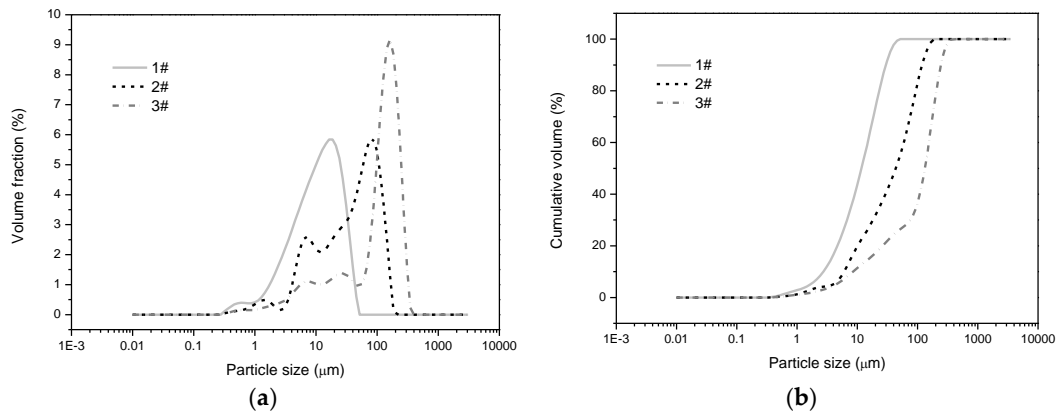


Figure 1. The coal particle size distribution results: (a) volume fraction; (b) cumulative volume.

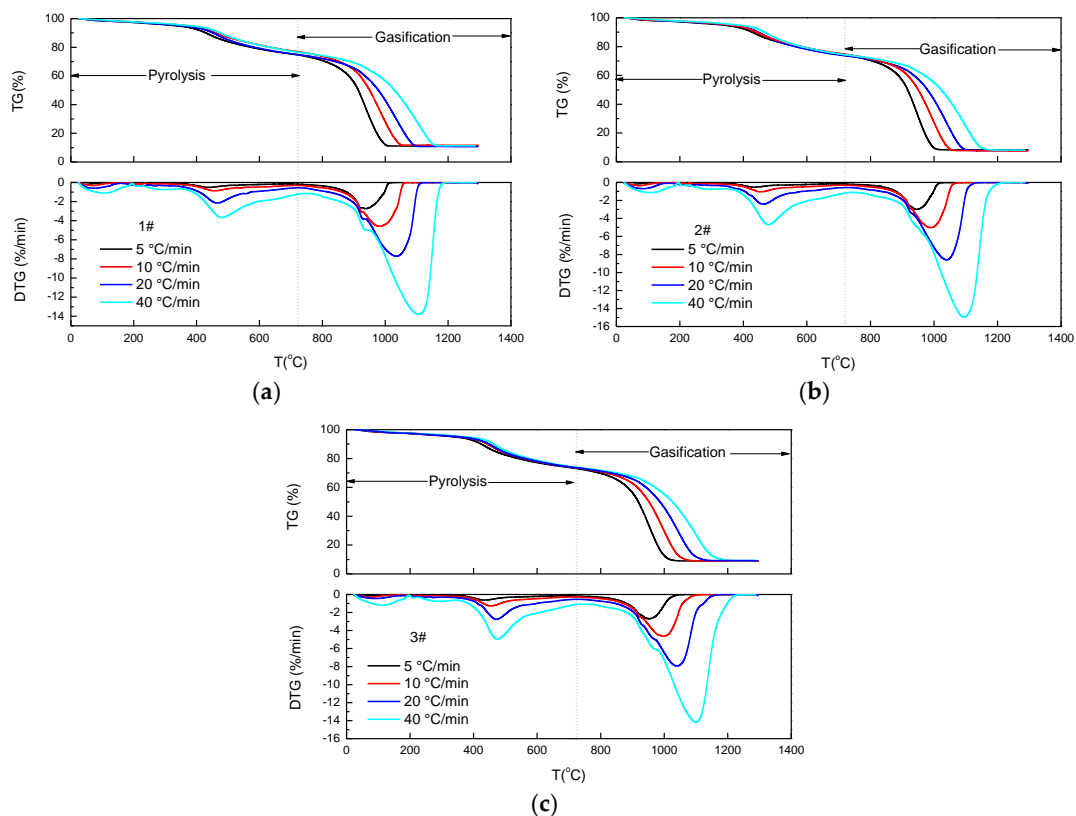


Figure 2. TG and DTG curves of coal samples under different heating rates: (a) 1#, (b) 2#, and (c) 3#.

The effect of particle size on TG curves can be seen in Figure 3. The weight loss curves for the three coal samples had similar trends. However, there were obvious differences in the final amount of solid residue when the temperature was higher than $1050\text{ }^{\circ}\text{C}$. The final solid residue amount for 1# was the largest, 3# was second, and the 2# had the smallest final solid residue amount, which was consistent with the results of the ash amount in the proximate analysis. One explanation for this is that mineral compositions in coal have high brittleness, whereas organic compositions in coal have good toughness. During the process of breaking large coal particles, mineral compositions were more easily

broken than organic compositions; therefore, more mineral compositions were abundant in the part of the coal sample with the small particle sizes after screening.

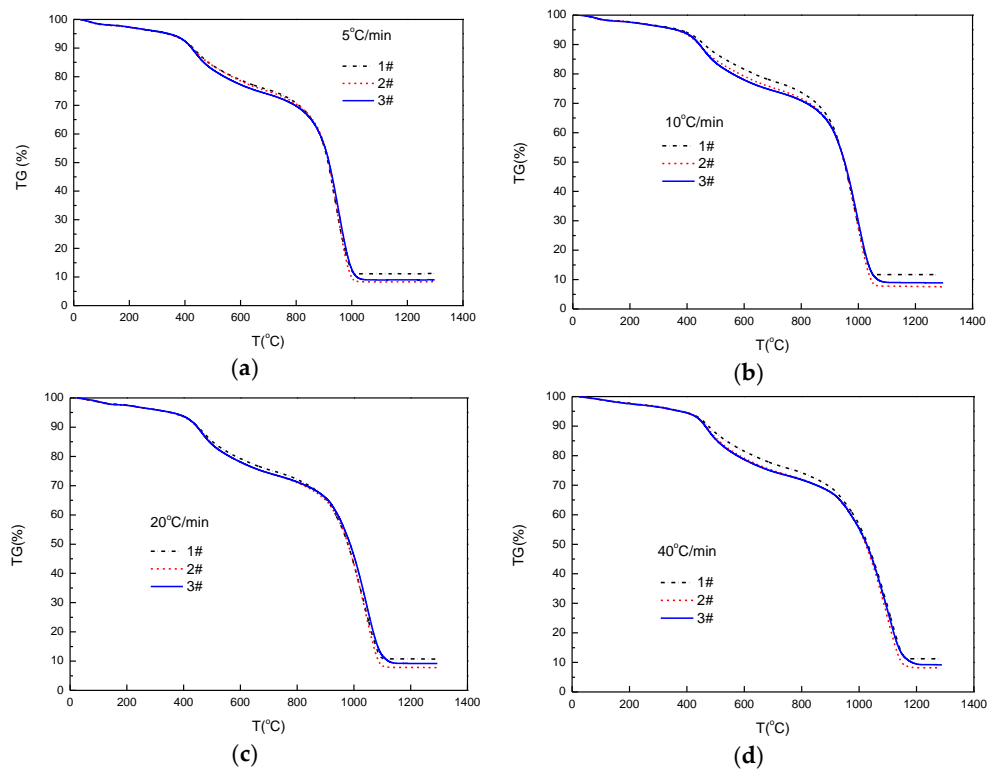


Figure 3. TG curves of coal samples with different particle sizes: (a) 5 K/min, (b) 10 K/min, (c) 20 K/min, and (d) 40 K/min.

4.3. Kinetic Analysis with Isoconversional Methods

The gasification conversion factor, α , can be expressed as follows:

$$\alpha = \frac{m_0 - m}{m_0 - m_\infty} \times 100\%, \quad (2)$$

where m_0 refers to the initial mass of the coal sample in the gasification stage, m is the real-time mass at some time of the gasification stage, and m_∞ is the final mass of the coal sample when the gasification is over.

The changes in the gasification conversion factor when the temperature was increased for the three Shenhua bituminous coal samples are shown in Figure 4. The gasification conversion factor increased slightly when the temperature was lower than 850 °C and the conversion curves nearly overlapped for the three coal samples with different particle sizes. Nevertheless, a rapid rise of the gasification conversion factor was found when the temperature was higher than 850 °C and visible differences were found for the three coal samples with different particle sizes. As for the effect of particle size on the gasification conversion factor, we found that α of 1# was the highest among the three coal samples at the same temperature, 2# was the second, and the 3# was the lowest.

The plot of $\ln(\beta/T^2)$ vs. $1/T$ for the constant gasification conversion factor (α) resulted in a straight line with the slope of $-E/R$ and intercept of $\ln(k_0R/E) + 0.6075$ as presented in Figure 5. The values of activation energy (E), pre-exponential factor (k_0), and correlation coefficient (R^2) estimated from the integral isoconversional model of Miura–Maki is presented in Table 3. Table 3 shows that the values of R^2 were all higher than 0.97, indicating that the integral isoconversional model of Miura–Maki was appropriate for estimation of the gasification kinetics of Shenhua bituminous coal.

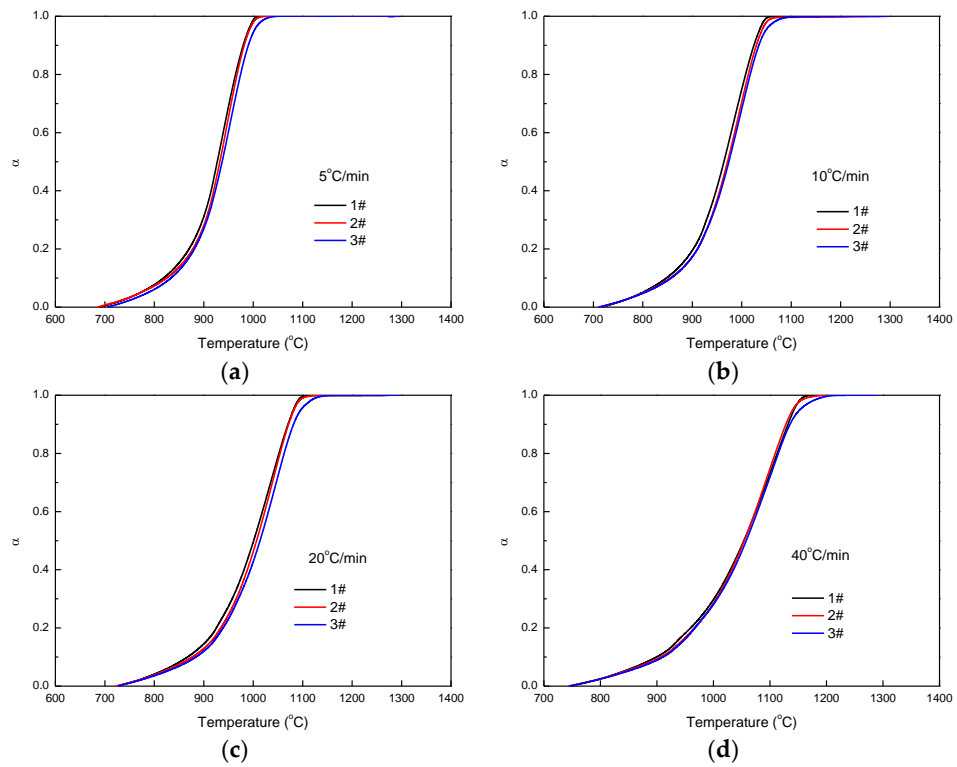


Figure 4. The gasification conversion factor for coal samples with different particle sizes: (a) 5 K/min, (b) 10 K/min, (c) 20 K/min, and (d) 40 K/min.

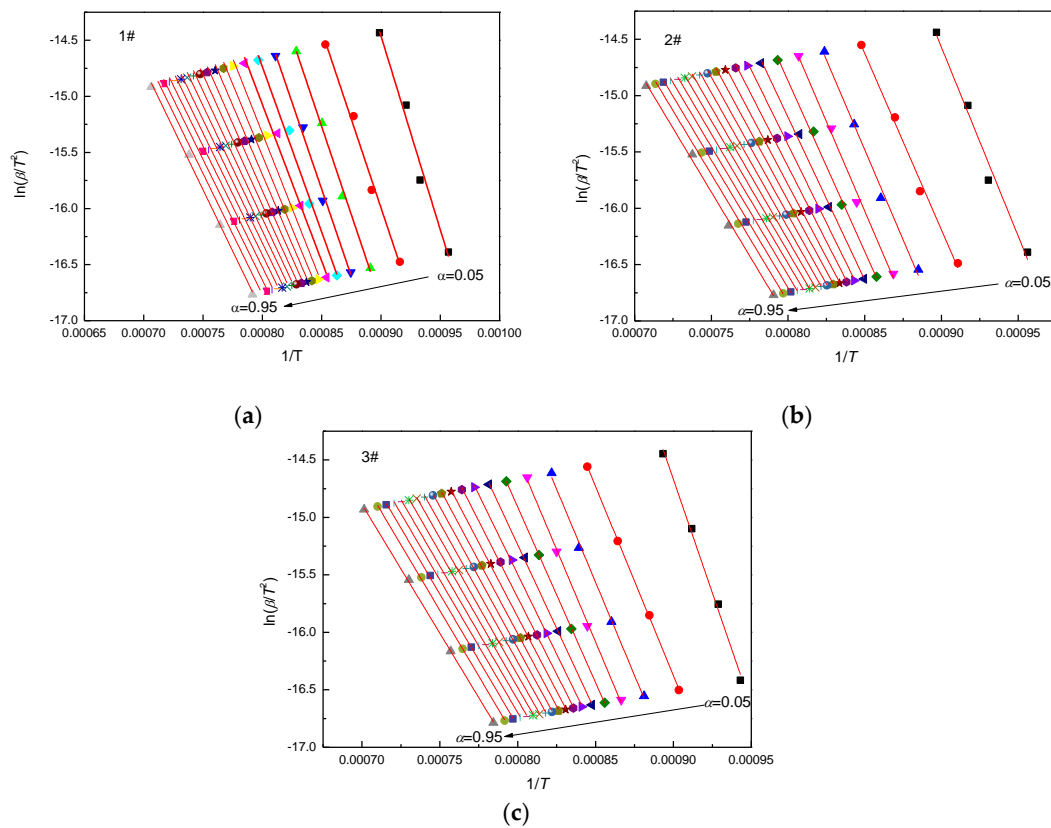
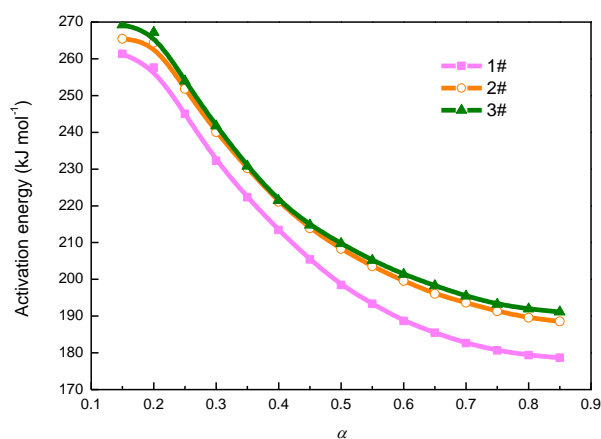


Figure 5. Graphical representation based on the integral isoconversional model of Miura–Maki for samples with different particle sizes: (a) 1#, (b) 2#, and (c) 3#.

Table 3. Kinetic parameters from the integral isoconversional model of Miura–Maki for coal samples with different particle sizes.

α	E (kJ mol ⁻¹)			k_0 (s ⁻¹)			R ²		
	1#	2#	3#	1#	2#	3#	1#	2#	3#
0.05	287.24	278.47	328.01	3.15×10^{11}	1.06×10^{11}	2.41×10^{13}	0.975	0.978	0.994
0.10	262.59	260.45	273.57	4.31×10^9	2.78×10^9	1.01×10^{10}	0.988	0.990	0.999
0.15	261.31	265.44	269.22	1.60×10^9	2.01×10^9	2.76×10^9	0.994	0.991	0.997
0.20	257.58	264.38	267.19	6.17×10^8	1.04×10^9	1.32×10^9	0.993	0.992	0.998
0.25	245.02	251.78	253.96	1.11×10^8	1.91×10^8	2.28×10^8	0.989	0.996	0.999
0.30	232.27	240.02	241.76	2.20×10^7	4.25×10^7	4.84×10^7	0.990	0.996	0.999
0.35	222.30	230.20	230.79	6.25×10^6	1.24×10^7	1.24×10^7	0.990	0.996	0.999
0.40	213.39	221.10	221.41	2.08×10^6	4.10×10^6	3.95×10^6	0.990	0.996	0.999
0.45	205.38	213.88	214.76	7.84×10^5	1.68×10^6	1.71×10^6	0.991	0.996	0.999
0.50	198.43	208.24	209.71	3.36×10^5	8.27×10^5	8.87×10^5	0.992	0.996	0.999
0.55	193.36	203.54	205.16	1.77×10^5	4.53×10^5	4.92×10^5	0.992	0.997	0.999
0.60	188.68	199.55	201.37	9.77×10^4	2.70×10^5	2.98×10^5	0.993	0.997	0.999
0.65	185.42	196.06	198.23	6.28×10^4	1.70×10^5	1.94×10^5	0.993	0.997	0.999
0.70	182.62	193.63	195.46	4.24×10^4	1.20×10^5	1.31×10^5	0.994	0.997	0.999
0.75	180.64	191.29	193.23	3.12×10^4	8.51×10^4	9.41×10^4	0.994	0.997	0.999
0.80	179.37	189.55	191.96	2.45×10^4	6.43×10^4	7.40×10^4	0.994	0.997	0.999
0.85	178.68	188.52	191.11	2.04×10^4	5.18×10^4	6.03×10^4	0.995	0.997	0.999
0.90	179.42	188.20	190.07	1.93×10^4	4.43×10^4	4.74×10^4	0.996	0.997	0.999
0.95	181.69	188.63	186.35	2.08×10^4	3.94×10^4	2.72×10^4	0.996	0.996	0.999

According to activation energy values using the integral isoconversional model of Miura–Maki, as shown in Figure 6, 1# had the lowest activation energy values, followed by 2#, and the largest was 3#. We concluded that the activation energy decreased with the decrease in particle size of the coal sample. As shown in Figure 7, the plot of logarithmic scales (base 10) for the pre-exponential factor vs. activation energy using values reported in Table 3 resulted in a straight line, indicating that there was a compensation effect between activation energy and pre-exponential factor.

**Figure 6.** The activation energy estimated using the integral isoconversional model of Miura–Maki for coal sample with different particle sizes.

4.4. Ash Fusibility of Coal with Different Particle Size

As shown in Table 4, the ash fusion temperatures decreased in the order of 1#, 2#, and 3#. The sample of 1# had the highest ash fusion temperatures (DT, ST, HT, and FT), while there was no significant difference as for the ash fusion temperatures between 2# and 3#. These results indicated that particle size had an impact on ash fusion temperatures and smaller particle size resulted in higher ash fusion temperatures.

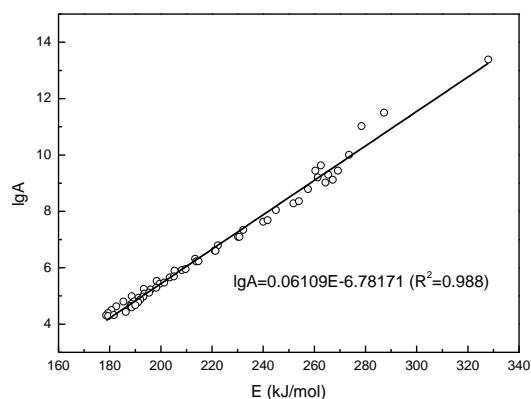


Figure 7. The plot of logarithmic scales (base 10) for the pre-exponential factor vs. activation energy using values reported in Table 1.

Table 4. Ash fusibility temperatures (AFTs) (°C) of Shenhua bituminous coal with different particle sizes.

Sample Number	DT/°C	ST/°C	HT/°C	FT/°C
1#	1220	1250	1270	1280
2#	1190	1200	1210	1220
3#	1180	1200	1210	1220

Ash fusion temperatures were highly dependent on its chemical composition. Table 5 shows the chemical compositions (wt %) of Shenhua bituminous coal ash with different particle sizes. On the basis of the assumption that similar compositions resulted in similar ash fusion temperatures, we found that the chemical compositions of coal ash had no significant difference with the increase in particle size.

Table 5. Chemical compositions (wt %) of Shenhua bituminous coal with different particle sizes.

Sample	SiO ₂	Al ₂ O ₃	Fe ₂ O ₃	CaO	MgO	TiO ₂	SO ₃	K ₂ O	Na ₂ O	P ₂ O ₅
1#	43.61	21.99	5.33	18.92	0.68	0.92	5.78	1.44	0.98	0.14
2#	39.36	19.66	6.00	20.60	0.65	0.93	9.86	1.18	1.22	0.12
3#	43.55	20.97	4.28	17.03	0.76	1.03	9.23	1.21	1.65	0.14

5. Conclusions

In this work, the effect of particle size on the gasification kinetics and the ash fusibility of Shenhua bituminous coal was investigated. The effect of particle size on TG curves was reflected in the final amount of solid residue when the temperature was higher than 1050 °C. The coal sample with the smallest particle size had the largest final solid residue amount, which was consistent with the results of the ash amount in the proximate analysis. The integral isoconversional model of Miura–Maki was proven to be appropriate for the estimation of the gasification kinetics of Shenhua bituminous coal. The calculated activation energy experienced a slow increase when the particle size of raw coal decreased. Small particle size resulted in higher ash fusion temperatures. Generally, coal samples with smaller particle size are more favourable for the gasification process.

Author Contributions: J.Z. and Z.W. conceived and designed the experiments; J.Z. performed the experiments, analyzed the data, and wrote the original draft. Z.W., R.Z. and J.W. reviewed and corrected the manuscript. All authors have read and agreed to the published version of the manuscript.

Funding: This research was funded by the National Key Research and Development Program of China (No. 2017YFB0601900), National Natural Science Foundation of China (Grant No. U1610254), Shandong Provincial Natural Science Foundation (Grant No. ZR2019BEE074), and “Director Innovation Fund of Key Laboratory of Biofuels, Chinese Academy of Sciences” (No. Y372081100).

Conflicts of Interest: The authors declare no conflict of interest.

References

1. Tian, B.; Qiao, Y.-Y.; Tian, Y.-Y.; Liu, Q. Investigation on the effect of particle size and heating rate on pyrolysis characteristics of a bituminous coal by TG-FTIR. *J. Anal. Appl. Pyrol.* **2016**, *121*, 376–386. [[CrossRef](#)]
2. Domenico, M.D.; Collazzo, G.C.; Pacioni, T.R.; Jose, H.J.; Moreira, R.F.P.M. Gasification of brazilian coal-chars with CO₂: Effect of samples' properties on reactivity and kinetic modeling. *Chem. Eng. Commun.* **2019**, *206*, 158–168. [[CrossRef](#)]
3. Labojko, G.; Kotyczka-Moranska, M.; Plis, A.; Sciazko, M. Kinetic study of polish hard coal and its char gasification using carbon dioxide. *Thermochim. Acta* **2012**, *549*, 158–165. [[CrossRef](#)]
4. Zhao, L.; Chu, X.; Cheng, S. Kinetic study of CO₂ gasification of coal chars. In *Advances in Chemical Engineering II, pts 1-4*; Liu, Z., Peng, F., Liu, X., Eds.; Trans Tech Publications: Stafa-Zurich, Switzerland, 2012; Volume 550–553, pp. 2754–2757.
5. Liu, L.; Cao, Y.; Liu, Q.; Yang, J. Experimental and kinetic studies of coal-CO₂ gasification in isothermal and pressurized conditions. *RSC Adv.* **2017**, *7*, 2193–2201.
6. Zeng, X.; Zheng, S.; Zhou, H. The phenomena of secondary weight loss in high-temperature coal pyrolysis. *Energy Fuels* **2017**, *31*, 10178–10185. [[CrossRef](#)]
7. Li, F.; Yan, Q.; Huang, J.; Zhao, J.; Fang, Y.; Wang, J. Lignite-char gasification mechanism in mixed atmospheres of steam and CO₂ at different pressures. *Fuel Process. Technol.* **2015**, *138*, 555–563. [[CrossRef](#)]
8. Fu, W.B.; Wang, Q.H. A general relationship between the kinetic parameters for the gasification of coal chars with CO₂ and coal type. *Fuel Process. Technol.* **2001**, *72*, 63–77. [[CrossRef](#)]
9. Kang, S.-H.; Ryu, J.-H.; Park, S.-N.; Byun, Y.-S.; Seo, S.-J.; Yun, Y. Kinetic studies of pyrolysis and char-CO₂ gasification on low rank coals. *Korean J. Chem. Eng.* **2011**, *49*, 114–119. [[CrossRef](#)]
10. Hanson, S.; Patrick, J.W.; Walker, A. The effect of coal particle size on pyrolysis and steam gasification. *Fuel* **2002**, *81*, 531–537. [[CrossRef](#)]
11. Zhu, W.; Song, W.; Lin, W. Effect of the coal particle size on pyrolysis and char reactivity for two types of coal and demineralized coal. *Energy Fuels* **2008**, *22*, 2482–2487. [[CrossRef](#)]
12. Kok, M.V.; Ozbas, E.; Karacan, O.; Hicyilmaz, C. Effect of particle size on coal pyrolysis. *J. Anal. Appl. Pyrol.* **1998**, *45*, 103–110.
13. Morris, R.M. Effect of particle-size and temperature on volatiles produced from coal by slow pyrolysis. *Fuel* **1990**, *69*, 776–779. [[CrossRef](#)]
14. Liu, J.; Jiang, X.; Shen, J.; Zhang, H. Pyrolysis of superfine pulverized coal. Part 1. Mechanisms of methane formation. *Energy Convers. Manag.* **2014**, *87*, 1027–1038. [[CrossRef](#)]
15. Liu, J.; Jiang, X.; Shen, J.; Zhang, H. Pyrolysis of superfine pulverized coal. Part 2. Mechanisms of carbon monoxide formation. *Energy Convers. Manag.* **2014**, *87*, 1039–1049. [[CrossRef](#)]
16. Liu, J.; Jiang, X.; Shen, J.; Zhang, H. Pyrolysis of superfine pulverized coal. Part 3. Mechanisms of nitrogen-containing species formation. *Energy Convers. Manag.* **2015**, *94*, 130–138. [[CrossRef](#)]
17. Liu, J.; Ma, Y.; Luo, L.; Ma, J.; Zhang, H.; Jiang, X. Pyrolysis of superfine pulverized coal. Part 4. Evolution of functionalities in chars. *Energy Convers. Manag.* **2017**, *134*, 32–46. [[CrossRef](#)]
18. Krishnamoorthy, V.; Pisupati, S.V. Fate of sulfur during entrained-flow gasification of pittsburgh no. 8 coal: Influence of particle size, sulfur forms, and temperature. *Energy Fuels* **2016**, *30*, 3241–3250. [[CrossRef](#)]
19. Jayaraman, K.; Kok, M.V.; Gokalp, I. Pyrolysis, combustion and gasification studies of different sized coal particles using TGA-MS. *Appl. Therm. Eng.* **2017**, *125*, 1446–1455. [[CrossRef](#)]
20. Miura, K.; Maki, T. A simple method for estimating $f(E)$ and $k_0(E)$ in the distributed activation energy model. *Energy Fuels* **1998**, *12*, 864–869. [[CrossRef](#)]
21. Chen, T.; Zhang, J.; Wu, J. Kinetic and energy production analysis of pyrolysis of lignocellulosic biomass using a three-parallel gaussian reaction model. *Bioresour. Technol.* **2016**, *211*, 502–508. [[CrossRef](#)]
22. Zhang, J.; Chen, T.; Wu, J.; Wu, J. Multi-gaussian-daem-reaction model for thermal decompositions of cellulose, hemicellulose and lignin: Comparison of N₂ and CO₂ atmosphere. *Bioresour. Technol.* **2014**, *166*, 87–95. [[CrossRef](#)]
23. Zhang, J.; Chen, T.; Wu, J.; Wu, J. A novel gaussian-daem-reaction model for the pyrolysis of cellulose, hemicellulose and lignin. *RSC Adv.* **2014**, *4*, 17513–17520. [[CrossRef](#)]

24. Zhang, J.; Chen, T.; Wu, J.; Wu, J. TG-MS analysis and kinetic study for thermal decomposition of six representative components of municipal solid waste under steam atmosphere. *Waste Manag.* **2015**, *43*, 152–161. [[CrossRef](#)]
25. Song, H.; Liu, G.; Zhang, J.; Wu, J. Pyrolysis characteristics and kinetics of low rank coals by TG-FTIR method. *Fuel Process. Technol.* **2017**, *156*, 454–460. [[CrossRef](#)]



© 2020 by the authors. Licensee MDPI, Basel, Switzerland. This article is an open access article distributed under the terms and conditions of the Creative Commons Attribution (CC BY) license (<http://creativecommons.org/licenses/by/4.0/>).